STEM CELLS AND DEVELOPMENT
Volume 00, Number 00, 2018

DOI: 10.1089/scd.2018.0031

Do Induced Pluripotent Stem Cell Characteristics Correlate with Efficient In Vitro Smooth Muscle Cell Differentiation? A Comparison of Three Patient-Derived Induced Pluripotent Stem Cell Lines

Yingying Zhou,[1,2,*] Gugene Kang,[3,*] Yan Wen,[1] Mason Briggs,[1] Vittorio Sebastiano,[3] Roger Pederson,[1] and Bertha Chen[1]

Human induced pluripotent stem cells (iPSCs) have the potential to repair/regenerate smooth muscle cells (SMCs) in different organs. However, there are many challenges in their translation to clinical therapies. In this study, we describe our observations of in vitro SMC differentiation in three iPSC lines derived from human fibroblasts using retroviral, episomal, and mRNA/miRNA reprogramming methods. We sought to elucidate correlations between differentiation characteristics and efficiencies that can facilitate large-scale production of differentiated cells for clinical applications, and to report differences in pluripotency marker expression in differentiated cells from different iPSC lines. A standardized SMC differentiation protocol was used to induce the $CD31^+/CD34^+$ vascular progenitor cell phenotype. These were sorted by magnetic-activated (MACS) and fluorescence-activated cell sorting (FACS), and then treated with PDGF-BB and smooth muscle growth medium for further differentiation into smooth muscle progenitor cells (pSMCs). The expression of SMC and pluripotency markers in early- and late-passage (P1 and P4) pSMCs was analyzed. A total of 36 differentiation runs was performed on the three patient iPSC lines. All pSMC populations expressed SMC markers and Ki67 consistent with the progenitor phenotype. Initial iPSC density correlated positively with the sorted cell FACS efficiency, and this correlation could be fit to a quadratic equation. We also observed that a specific ''honeycomb'' pattern of the starting cultured iPSCs cultured correlated with higher efficiency in all three iPSC lines. Pluripotency marker expression decreased significantly to nearly undetectable levels in all three lines. There was no significant change in SMC and pluripotent marker expression between passage 1 and 4. In summary, our observations suggest that the method of iPSC reprogramming does not affect iPSC differentiation into pSMCs. Protocol efficiency can be modeled mathematically and coupled with the initial ''honeycomb'' cell pattern to optimize production of large cell numbers for clinical therapies.

Keywords: iPSCs, smooth muscle cell progenitors, differentiation efficiency, cultured iPSC pattern, pluripotency markers

Introduction

Human induced pluripotent stem cells (iPSCs) derived from adult somatic cells by genetic reprogramming methods are capable of self-renewal and differentiation [1]. iPSCs, like embryonic stem cells, can be induced to differentiate into different types of mature functional cells in vitro. Thus, iPSCs can be used to produce homogenous populations of any cell type necessary for regenerative therapies, specifically, progenitor cells, which are difficult to harvest from adult tissues.

Smooth muscle cells (SMCs) originating from the mesoderm during embryogenesis make up the nonstriated muscle network in major blood vessels, lung, as well as the central layers of many hollow organs [2]. They are essential for the proper maintenance of organ function and blood pressure. Many studies on iPSC-derived smooth muscle progenitor cells (pSMCs) in tissue regeneration are under way. To date, published data support the concept that these progenitor cells may have the potential to repair the dysfunction of smooth muscle in many different systems, including the urinary system [3,4].

[1]Department of Obstetrics/Gynecology, Stanford University School of Medicine, Stanford, California.
[2]Department of Obstetrics/Gynecology, Shengjing Hospital, China Medical University, Shenyang, People's Republic of China.
[3]Institute for Stem Cell Biology & Regenerative Medicine, Stanford University School of Medicine, Stanford, California.
*These authors should be considered co-first authors of this article.

While these patient-specific stem cells and their derivatives may be able to bypass immunological limitations and ethical issues regarding pluripotent stem cells, many challenges must be addressed before clinical use.

The generation of therapies from pluripotent stem cells employs laboratory methods for cell generation, maintenance, and expansion that increase the risk of genetic instability, epigenetic modification, and generation of tumorigenic cells. iPSCs were initially established by introducing transcription factors, such as *OCT4*, *SOX2*, *NANOG*, and *KLF4* or *LIN28*, by retrovirus or lentivirus transfection [5,6]. This method risks incorporation of foreign genes into the cell, which increases the risk of mutation and tumorigenicity [7]. One strategy to minimize this risk is to use nonviral and nonintegrative methods of reprogramming, such as episomal and mRNA/miRNA reprogramming, to generate iPSCs from somatic cells [8–11].

Cell purification methods, such as magnetic-activated cell sorting (MACS) [12] and fluorescence-activated cell sorting (FACS) [13], can also be applied to minimize tumorigenic potential and generate homogenous cell populations. We have tested combinations of reprogramming and cell sorting methodologies to produce homogenous pSMC populations [14,15]. However, the yield from the starting population of iPSCs was inconsistent and insufficient for large-scale clinical production.

Given these significant barriers to clinical translation, tumorigenicity, and inconsistent differentiation yield, we sought to correlate differentiation characteristics with differentiation efficiency of an established smooth muscle differentiation protocol and examine tumorigenic impurities in pSMCs derived from three different iPSC reprogramming methodologies (retrovirus vector transfection, episome, and mRNA/miRNA), to better inform ongoing efforts in translation of stem cell technologies into therapies.

Materials and Methods

Reprogramming and maintenance of iPSC

Institutional Review Board of the Stanford University School of Medicine and the Stanford University Stem Cell Research Oversight Committee approved this study. Written informed consents were obtained from all subjects. Three human iPS cell lines derived with their fibroblasts were investigated in this study. The fibroblasts—isolated from a 41-year-old healthy woman (episomal iPSC line), a 46-year-old healthy woman (retroviral iPSC line), and a 18-year-old woman (mRNA/miRNA iPSC line)—were each cultured in 80% Dulbecco's modified Eagle's medium (DMEM; Invitrogen, Carlsbad, CA) and 20% fetal bovine serum (Invitrogen) at 37°C in an atmosphere of 95% air and 5% CO_2, as described previously [3]. Luciferase (Luc)-tagged retrovirus iPSC line was reprogrammed to iPSCs through viral transduction of the transcription factors Oct3/4, Sox2, Klf4, and c-Myc, and the episomal iPSC line was reprogrammed to iPSCs using nonintegrating episomal plasmids (Invitrogen) [4].

The mRNA/miRNA iPSC line was reprogrammed with modified miRNA reprogramming method as described by Bilousova et al. (unpublished). mRNA encoding Oct4, Klf4, Sox2, c-Myc, and Lin28 were co-transfected with a mixture of several miRNAs into the fibroblasts to induce iPSCs. Briefly, human fibroblasts were seeded at a density of 3,000 cells/well in a six-well dish, precoated with recombinant human Laminin521(rhLaminin521, BioLamina, Matawan, NJ) in a reprogramming medium composed of DMEM/F12 (DMEM/Nutrient Mixture F-12), 20% knockout serum replacement (Thermo Fisher, Waltham, MA), 0.05 mM NEAA, 1 mM glutamax (Gibco, Waltham, MA), 55 mM 2-mercaptoethanol, 50 μg/mL ascorbic Acid, and Pen/Strep. The reprogramming medium was supplemented with 100 ng/mL bFGF and 200 ng/mL B18R (eBioscience, Waltham, MA) throughout the protocol. The next day, the medium was replaced with reprogramming medium equilibrated at 5% O_2 overnight before use. RNA transfections were carried out using Lipofectamine RNAiMAX (Invitrogen) cationic lipid delivery vehicles; 100 ng/μL of mRNA was diluted 5× in Opti-MEM basal media (Invitrogen) and mixed together with 5 μL of RNAiMAX per microgram of mRNA, while 5 μM miRNA was diluted 8.33× and mixed with 1 μL of RNAiMAX per 6 picomoles of miRNA. These complexes were then incubated for 15 min at room temperature (RT) before being dispensed into the culture media. Transfections were repeated every other day for seven total transfections, and media were changed 20–24 h after each transfection. Individual colonies were selected approximately 15–18 days after the first transfection for further clonal expansion. G-banded karyotyping of mRNA-iPSCs was performed as previously described by WiCell [4] (Supplementary Fig. S1; Supplementary Data are available online at www.liebertpub.com/scd). The pluripotency markers, octamer binding transcription factor 4 (*OCT4*), sex-determining region Y box 2 (*SOX2*), stage-specific embryonic antigen 3 (*SSEA3*), stage-specific embryonic antigen 4 (*SSEA4*), *TRA-1-60*, and *TRA-1-81* in mRNA-iPSCs were determined by quantitative PCR and immunochemistry [16]. iPSCs were maintained on Matrigel-precoated dishes (BD Biosciences, San Diego, CA) in mTeSR medium (StemCell Technologies, Vancouver, BC).

Cell culture and differentiation

Human bladder SMCs (bSMCs) (Lonza, Allendale, NJ) were cultured in 90% DMEM and 10% fetal bovine serum at 37°C in an atmosphere of 95% air and 5% CO_2.

Human pSMCs were differentiated from the three iPSC lines using a modified, feeder cell-free, vascular progenitor protocol as previously described [3,4,14,17]. Briefly, the iPSCs were seeded at a density of 5,000–20,000 cells per cm^2 of a 10-cm dish precoated with Matrigel in mTeSR supplemented with Thiazovivin (2 μM; Cayman Chemical Company, Ann Arbor, MI). After 24–72 h in culture, images were recorded. The iPSCs were then cultured in chemically defined media (RPMI 1640 with 1 mM glutamax, 1% nonessential amino acids, 0.1 mM β-mercaptoethanol, 1% penicillin and streptomycin [Life Science Technology, Inc.], 1% ITS [Sigma-Aldrich]) supplemented with Activin A (50 ng/mL), BMP4 (50 ng/mL; PeproTech, Rocky Hill, NY), and 2.5 μM/mL GSK 3 inhibitor, CHIR99021 on day 0, 2.0 μM/mL CHIR99021 on day 1 (Cayman Chemical Company), followed by basic fibroblast growth factor (50 ng/mL) and vascular endothelial growth factor (40 ng/mL; PeproTech) from day 2 to 12–14 days.

The differentiated cells were dissociated with Accutase (Innovative Cell Technologies, San Diego, CA) and prepared for MACS and FACS of $CD31^+/CD34^+$ vascular progenitor cells (VPCs) as described previously [3]. Briefly,

the cells were first immunolabeled with CD34 microbeads for MACS (Miltenyi Biotec, Auburn, CA), and magnetic labeling was performed strictly according to the manufacturer's instructions. The magnetically labeled $CD34^+$ VPCs were obtained by positive selection. The $CD34^+$ VPCs sorted by MACS were immediately blocked with mouse IgG (R&D Systems, Inc., Minneapolis, MN) for 10 min and stained with FITC mouse anti-human CD31 and PerCP-Cy5.5 mouse anti-human CD34 antibodies (BD Biosciences) for 30 min at 4°C. The $CD31^+/CD34^+$ cells were sorted on a FACS Aria II (BD Biosciences) (Supplementary Fig. S2). Postsorting, the smooth muscle progenitor cells (pSMCs), passage 0 (P0), were expanded on collagen IV-precoated plates (BD Biosciences) in smooth muscle cell growth medium (SMGS; Invitrogen) supplemented with recombinant human platelet-derived growth factor-BB (10 ng/mL, PDGF-BB; PeproTech) to yield pSMCs. The pSMCs were passed with 0.05% Trypsin with EDTA (Thermo Scientific, Fremont, CA) when they reached 80–90% confluency. Each passage of pSMCs was divided into two groups during passing, one of them was for pluripotency and SMC marker detection, and the other one was for cell expansion. One group of P4 cells was prepared for pluripotency and SMC marker detection, and the other one was terminally differentiated to mature SMCs by culturing in smooth muscle differentiation medium (Invitrogen) for further SMC characterization and contraction assay (below).

Comparative relative quantification real-time PCR

The expression of representative mRNA in cells was analyzed by quantitative real-time PCR. RNA extraction was carried out with RNA-STAT-60 reagent (Tel-Test, Inc., Friendswood, TX). cDNA was generated from total RNA as described previously [18]. PCR primers used to amplify cDNA are shown in Table 1 [3,18,19]. QPCR (real-time quantification PCR) was carried on the Mx3005P Mutiplex Quantitative PCR System with MxPro QPCR software (Stratagene, La Jolla, CA). Brilliant SYBR Green QPCR Master Mix (Stratagene) was used to perform PCR. The amplifications were done following a 10-min hot start at 95°C in a three-step protocol with 30 s denaturation (94°C), 1 min annealing (55°C), and extension at 72°C for 30 s. Forty cycles were performed. *GAPDH* was used as an endogenous reference against which the different template values were normalized. All PCR were performed in duplicate. Ct (cycle of threshold) method was used for quantification. Relative quantification of the representative gene, corrected for the quantity of normalizer gene (*GAPDH*), was divided by one normalized control sample value (calibrator, bSMCs for pSMCs and H9-ESCs for iPSCs) to generate the relative quantification to calibrator (Rel.Quant. to Cal.). MxPro QPCR software was used for the calculations.

Table 1. Primers for Quantification Real-Time Polymerase Chain Reaction

Primers	*Sequences*
SMTN	F: GATGATGGCCTTGCCAAACTG
	R: CTGGATGCGTCCTAGGTCAT
SMA	F: AAAAGACAGCTACGTGGGTGA
	R: GCCATGTTCTATCGGGTACTTC
SM22	F: ATCCCAACTGGTTCCCTAAGAA
	R: CCCATCTGTAACCCGATCACG
CNN1	F: TGTGCAGACGGAACTTCAG
	R: GGTTGAAGTGAGCAGAGGAC
MYH11	F: CGCCAAGAGACTCGTCTGG
	R: TCTTTCCCAACCGTGACCTTC
ELN	F: AGGCAAACCTCTTAAGCCAGTTCC
	R: CAGACACTCCTAAGCCACCAACTC
OCT4	F: TCGAGAACCGAGTGAGAGG
	R: GAACCACACTCGGACCACA
SOX2	F: AGCTACAGCATGATGCAGGA
	GGTCATGGAGTTGTACTGCA
NANOG	F: ATGCCTCACACGGAGACTGT
	R: AAGTGGGTTGTTTGCCTTTG

Immunofluorescence staining

SMC markers for immunofluorescence staining were chosen from previous publications (Marchand et al. [14] and Bajpai et al. [20]). The cells were plated on an eight-well chamber slide for 24–48 h. The cells were fixed with 4% PFA/PBS (paraformaldehyde/phosphate buffer solution) for 10 min at room temperature and then washed with PBS thrice and treated with 0.5% Triton X-100in PBS for 5 min. The slides were then washed twice with 0.01% Tween in Tris-buffered Saline (TBS-T). After blocking with 1% bovine serum albumin (BSA) in TBST, the slides were incubated overnight at 4°C with primary antibody for Ki-67 (1:50, rabbit monoclonal antibody; Novus); SMC markers (SM-22, 1:20, goat monoclonal antibody; Abcam), α smooth muscle actin (α-SMA, 1:200, rabbit monoclonal antibody; Abcam), CNN1 (1:100, rabbit monoclonal antibody; Abcam), and smoothelin (SMTN, 1:50, rabbit monoclonal antibody; Santa Cruz); and pluripotent markers (TRA-1-60, 1:200, mouse monoclonal antibody, IgM; Millipore), TRA-1-81 (1:200, mouse monoclonal antibody, IgM; Millipore), SSEA3 (1:200, rabbit monoclonal antibody; Millipore), SSEA4 (1:200, mouse monoclonal antibody; Millipore), SOX2 (1:25, rabbit monoclonal antibody; Santa Cruz), and OCT4 (1:80, rabbit monoclonal antibody; Abcam). After washing with TBST for 10 min, thrice at room temperature, the slides were incubated with secondary antibody for 1 h at room temperature: Alexa 594-conjugated goat anti-rabbit IgG (1:300; Invitrogen), FITC-conjugated donkey anti-goat IgG (1:300; Santa Cruz), Alexa 488-conjugated goat anti-rabbit IgG (1:300; Invitrogen), and Alexa 594-conjugated goat anti-mouse IgM (1:300; Invitrogen). The slides were washed with TBST for 10 min thrice and then counterstained with DAPI (0.5 μg/mL DAPI/TBST) for 10 min. The slides were mounted with VECTASHIELD (H-1000; VECTOR, Inc., Burlingame, CA) and photographed with AxioCam (Zeiss, Oberkochen, Germany). The deletion of the primary antibody from the blocking buffer was used as a negative control. The pSMCs were characterized by staining for α-SMA, CNN1, SM22α, SMTN, and desmin. Ki67 staining was used to show proliferation.

Terminal SMCs were characterized by staining for SMTN, α-SMA, CNN1, SM22α, desmin (1:40, mouse monoclonal antibody; Sigma), and elastin (1:20, rabbit monoclonal antibody; Millipore)

Contraction assay

Terminal SMCs were characterized functionally with a carbachol contraction assay as described previously [14]. In

brief, P4 pSMCs were cultured for 7 days in smooth muscle differentiation medium (SMDS; Invitrogen), supplemented with 2.5 ng/mL TGFβ1 (Santa Cruz Biotechology, CA) to achieve terminal SMC differentiation. The cells were then treated with 100 mM carbachol (Sigma-Aldrich) in SMDS to induce cell contraction. The images of contraction were recorded with a Nikon Biostation IM (Nikon, Tokyo, Japan) every minute for 10 min. Percent change in cell surface area with carbachol treatment compared to no treatment was calculated.

Statistics

Data were analyzed using SPSS version 21 (SPSS, Inc., Chicago, IL). Results are shown as mean ± SEM. One sample Kolmogorov–Smirnov test was used to verify a normal distribution. Double-sided Student's *t* test and Kruskal–Wallis one-way ANOVA on ranks, followed by Wilcoxon–Mann–Whitney test were used to compare variables. Pearson and Spearman correlation coefficient were used to analyze the relationship between two groups of data. Curve fitting was applied to FACS efficiency data. $P < 0.05$ was considered to be statistically significant.

Results

Generation and characterization of iPSC lines from fibroblasts

Three iPSC lines were successfully generated by using either single polycistronic retroviral vector or episome, encoding Oct4, Klf4, Sox2, and cMyc, or mRNA encoding Oct4, Klf4, Sox2, cMyc, and Lin28. All three methods produced normal karyotype iPSCs. Immunofluorescence staining showed that the pluripotency markers, *OCT4*, *SOX2*, *SSEA-3*, *SSEA-4*, *TRA-1-60*, and *TRA-1-80*, were all positive. In addition, the mRNA expression level of pluripotency markers (*NANOG*, *SOX2*, *OCT4*, *cMYC*, *KLF4*, and *hTERT*) in all three iPSC lines was similar to that of H9 human embryonic stem cells (H9 hESCs, positive control). Taken together, these tests confirmed successful reprogramming of patient fibroblasts into iPSCs for each of the methods used.

Generation of smooth muscle progenitor cells from the iPSC lines

Each of the three patient iPSC lines was expanded and subjected to the same pSMC differentiation protocol as illustrated in Fig. 1. Several differentiation batches were performed for each line (16 batches using the retroviral reprogrammed iPSC line, 14 batches using the episomal reprogrammed line, and 6 batches using the mRNA/miRNA reprogrammed line). Proper differentiation into the SMC phenotype was confirmed for all lines by positive immunofluorescence staining of SMC proteins, SMTN, α-SMA, transgelin (SM22), and calponin (CNN1), and negative staining of the pluripotency markers, OCT4, TRA-1-60, and TRA-1-81 (Fig. 2A–C). Ki67, a marker for cell proliferation, was also positive in all the pSM cells, consistent with the progenitor, proliferative phenotype.

In addition to smooth muscle marker expression, functional testing was done to further confirm proper SMC differentiation. The pSMCs derived from each iPSC line were further differentiated into terminal SMC and tested for their ability to contract with carbachol stimulation compared to positive control (human bSMCs). SMCs differentiated from all three iPSC lines contracted similarly during the 10-min period after carbachol treatment (Fig. 3A), and when compared to human bSMCs (positive controls, bSMCs). More

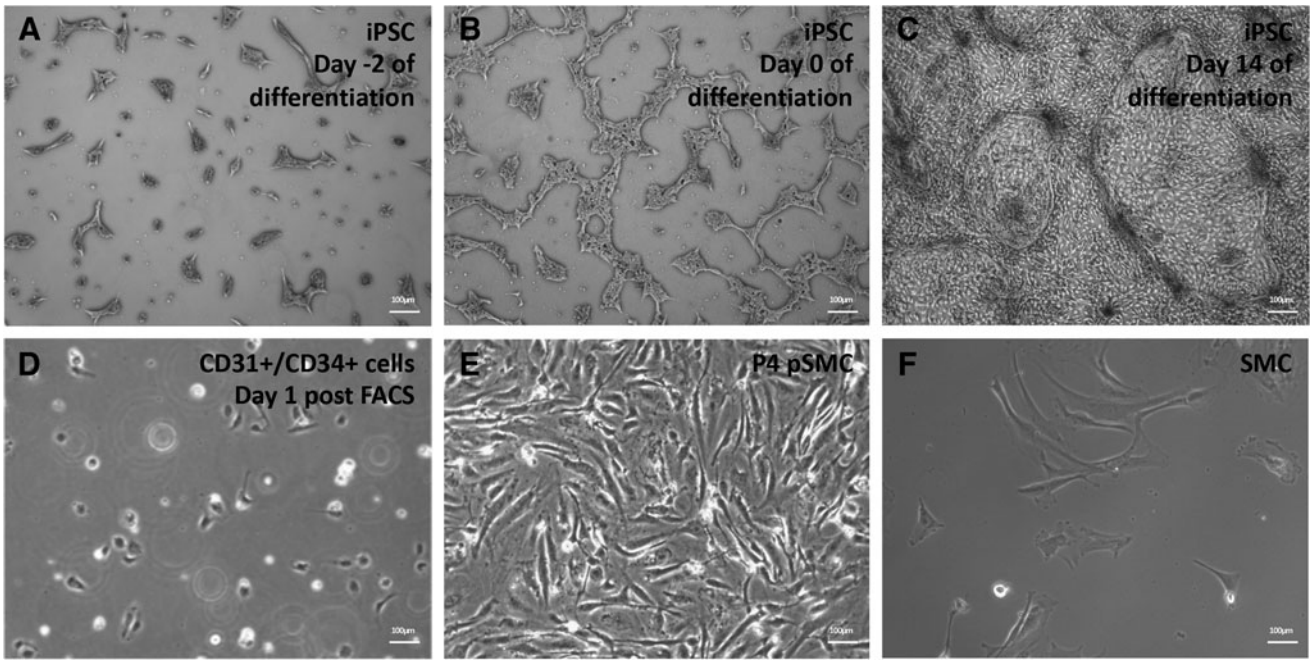

FIG. 1. Process of differentiation from iPSCs (day 2) to mature SMCs. **(A)** Cell pattern of iPSC 2 days before differentiation. **(B)** Cell pattern of iPSC on the differentiation day. **(C)** Cell pattern on the FACS day (14 days after differentiation). **(D)** Sorted $CD31^+/CD34^+$ cells after MACS and FACS. **(E)** Passage 4(P4) pSMCs were obtained after sorted cells being passed 4 times. **(F)** After culturing in smooth muscle differentiation medium mature SMCs were harvested. Scale bar = 100 μm. iPSC, induced pluripotent stem cell; pSMC, smooth muscle progenitor cells; SMCs, smooth muscle cells.

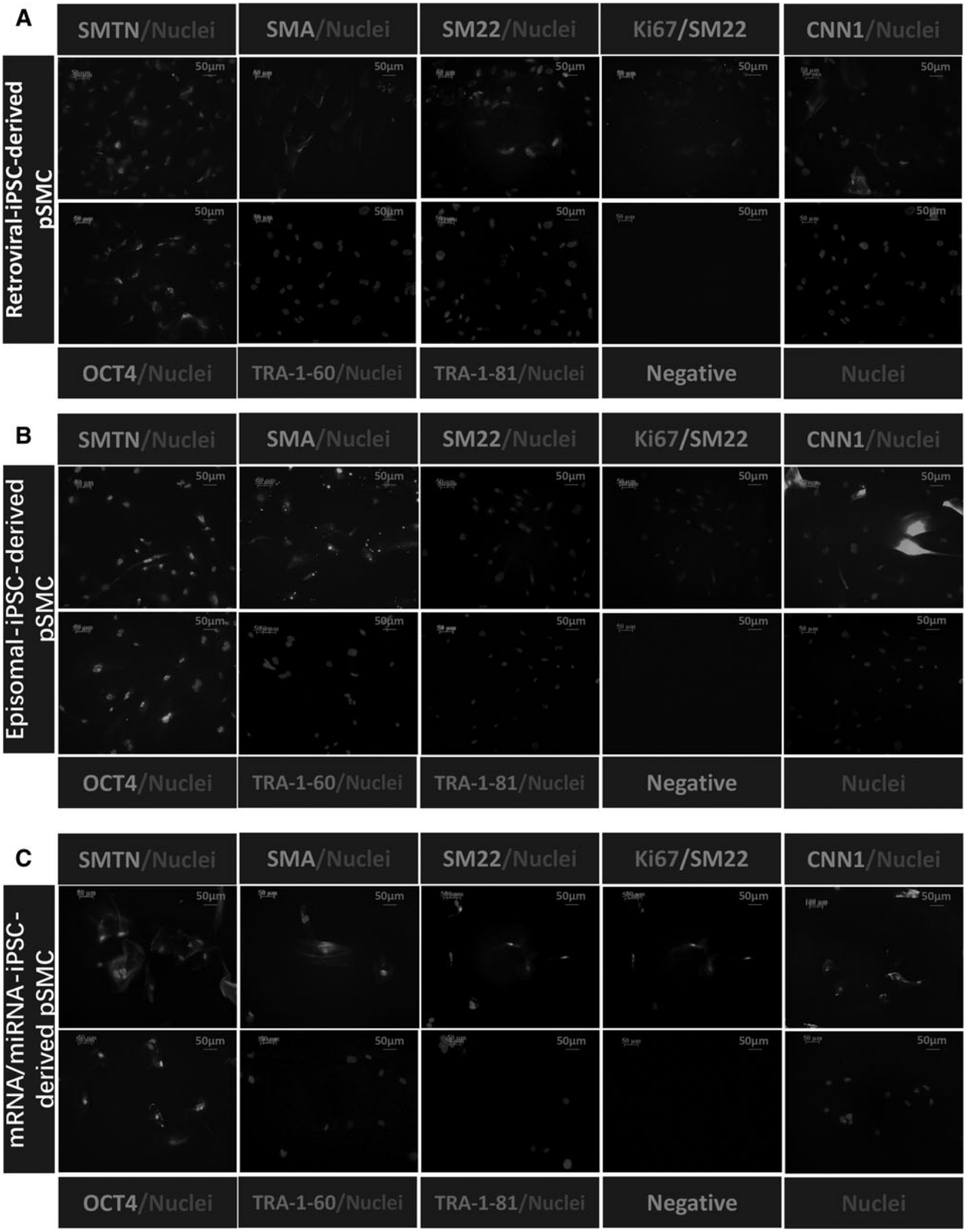

FIG. 2. **(A–C)** Characterization of pSMCs derived from MACS and FACS sorted VPCs. **(A)** pSMC derived from retroviral iPSC-differentiated VPCs, **(B)** pSMC derived from episomal iPSC-differentiated VPCs, **(C)** pSMC derived from mRNA/miRNA iPSC-differentiated VPCs. All three groups of cells were positive for SMTN, αSMA, SM22, calponin, and Ki67. Scale bar = 50 μm. pSMC, smooth muscle progenitor cells; FACS, fluorescence-activated cell sorting; MACS, magnetic-activated cell sorting; VPCs, vascular progenitor cells that are $CD31^{+}/34^{+}$.

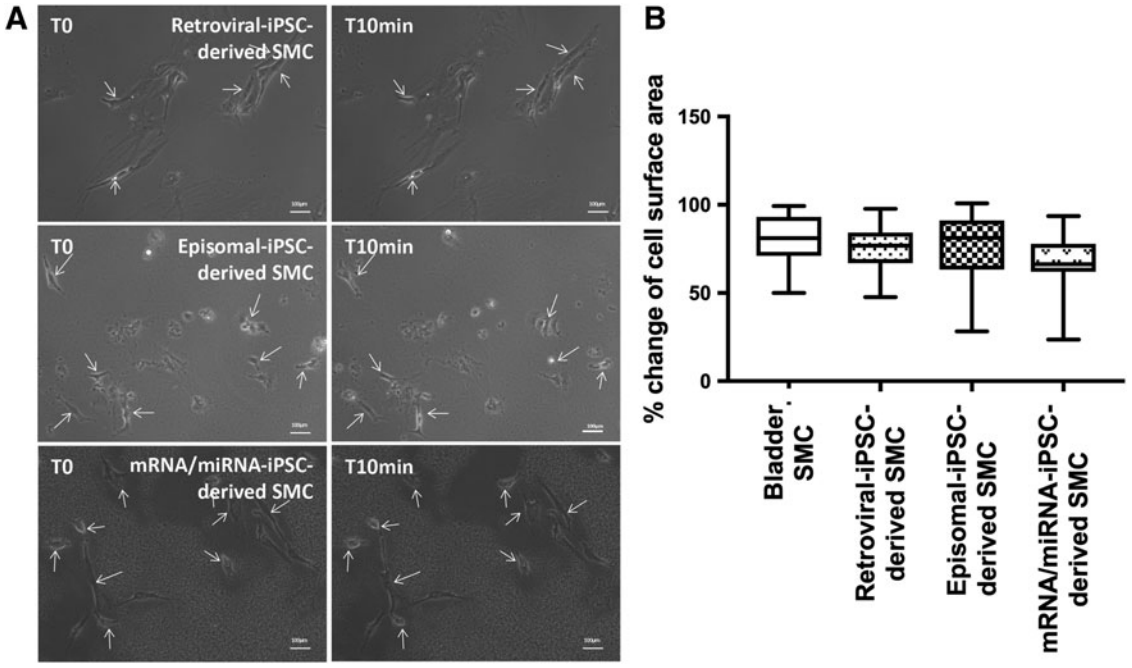

FIG. 3. Functional characterization of mature SMCs derived from iPSC. **(A)** SMCs treated with 100 mM carbachol demonstrated ability to contract, **(B)** retroviral iPSC-derived SMCs, episomal iPSC-derived SMCs, and mRNA/miRNA iPSC-derived SMCs showed a 20–30% change in surface area after contraction, human bladder SMC served as control. Scale bar = 100 μm. *Arrow* shows the change of a SMC cell surface before and after being treated with carbachol in the same group.

than 50% of the cells contracted with carbachol, resulting in a 20–30% change in surface area after contraction ($n = 50$) (Fig. 3B).

Relationship between the initial iPSC density before differentiation and the CD31$^+$/CD34$^+$ cell FACS efficiency

One of the intermediate steps in the differentiation protocol is the establishment of a population of VPCs characterized by the co-expression of CD31 and CD34. These cells are sorted out from the general cell population by FACS and are then treated with the smooth muscle growth medium for further differentiation into pSMCs. We used the percentage yield of CD31$^+$/34$^+$ cells sorted by FACS as parameter for differentiation efficiency, that is, higher CD31$^+$/34$^+$ yield represents higher differentiation efficiency.

The distribution of CD31$^+$/CD34$^+$ cell FACS efficiencies for all the differentiation runs using the retroviral and episomal iPSC lines conformed to a normal distribution according to the one sample Kolmogorov–Smirnov test. Spearman correlation tests indicated a positive correlation between starting iPSC density before differentiation and CD31$^+$/CD34$^+$ cell FACS efficiency in the retroviral iPSC group ($n = 16$, correlation coefficient = 0.528, $P < 0.05$) and in the episomal iPSC group ($n = 14$, correlation coefficient = 0.694, $P < 0.05$) (Table 2). Curve fitting for starting iPSC density and efficiency (Table 3) revealed that the quadratic curve was the best fit (retroviral iPSC line, $P < 0.05$; episomal iPSC line, $P < 0.05$, Fig. 4). Curve fitting was not performed for the mRNA/miRNA iPSC group due to the small number of differentiation runs (Table 2).

Correlation between initial cultured iPSC pattern and CD31$^+$/CD34$^+$ cell FACS efficiency

We observed that a ''honeycomb-like'' growth pattern of the cultured iPSCs that correlated with increased efficiency of CD31$^+$/CD34$^+$ conversion and, therefore, yield (Fig. 5). To assess the relationship between this pattern and CD31$^+$/CD34$^+$ FACS efficiency, the FACS efficiencies from each iPSC group were grouped into lower efficiency and higher efficiency subgroups. The cutoff for each group was determined

Table 2. Description of Correlation Between Initial Density Before Differentiation and C31$^+$/CD34$^+$ Cell Fluorescence-Activated Cell Sorting Efficiency in Three Induced Pluripotent Stem Cell Lines

	Mean ± SEM			
Groups	*Initial density before differentiation (k/cm^2)*	*Efficiency (%)*	*Correlation coefficient (ρ)*	P *value*
Retroviral iPSC differentiation ($n = 16$)	9.64 ± 1.13	32.29 ± 3.03	0.528	<0.05
Episomal iPSC differentiation ($n = 14$)	13.31 ± 1.21	19.05 ± 1.07	0.694	<0.05
mRNA/miRNA iPSC differentiation ($n = 6$)	30.10 ± 1.49	16.31 ± 1.95	–0.178	= 0.1

iPSC, induced pluripotent stem cell.

Table 3. Curve Fitting Analysis to Examine the Determinant of Efficiency as Measured by Initial Induced Pluripotent Stem Cell Density

	P *value*										
iPSCs groups	*Linear*	*Logarithmic*	*Inverse*	*Quadratic*	*Cubic*	*Compound*	*Power*	*S*	*Growth*	*Exponential*	*Logistic*
Retroviral ($n=16$)	<0.05	<0.05	<0.05	**<0.05**	0.1	<0.05	<0.05	<0.05	<0.05	<0.05	<0.05
Episomal ($n=14$)	<0.05	<0.05	<0.05	**<0.05**	<0.05	<0.05	<0.05	<0.05	<0.05	<0.05	<0.05
mRNA/miRNA ($n=6$)	0.4	0.4	0.4	0.6	0.6	0.4	0.4	0.4	0.4	0.4	0.4

The *bold P* value means the quadratic curve was fit for the relationship between iPSC density and efficiency and in compliance with the fact.

by ranking all the efficiencies from low to high and splitting the group in half—the lower half was classified as the lower efficiency group and the higher half, the higher efficiency group.

The difference in $CD31^+/CD43^+$ FACS efficiency between lower and higher efficiency subgroups was significant in retroviral, episomal, and mRNA/miRNA ($P<0.05$, $P<0.05$, and $P<0.05$) iPSC groups. The starting cell density was similar for all iPSC groups that underwent the pSMC differentiation protocol. Greater than 50% of higher efficiency subgroups exhibited the ''honeycomb-like'' pattern, while none of the lower efficiency subgroups exhibited this pattern. This behavior was also observed among the mRNA/miRNA iPSC differentiation runs, but the number of runs was too few for statistical analysis (Table 4).

Persistence of smooth muscle progenitor cell phenotype over time

pSMCs expressed SMC markers (*SMTN*, *SMA*, *SM22*, and *CNN1*) at passage 1 and passage 4. This was consistent for all pSMCs differentiated from the retroviral ($n=9$), episomal ($n=6$), and mRNA/miRNA ($n=3$) iPSC lines. We also evaluated the gene expression of pluripotency makers (*OCT4*, *SOX2*, and *NANOG*) by quantitative polymerase chain reaction in a representative number of pSMC batches to examine the change with increasing passages. Human bladder SMCs (bSMCs) served as the calibrator (Fig. 6). There was no significant difference in the expression of SMC markers between passage 1 and 4 in pSMCs derived from the three patient iPSC lines, suggesting stability of cell phenotype regardless of iPSC reprogramming method.

For the pluripotency marker comparison, the gene relative expression of the three pluripotency markers in the original iPSCs served as calibrator (Fig. 6). Pluripotency marker expression in all pSMC groups, regardless of passage number, was significantly decreased compared to the expression in their original iPSC state (retroviral group, $n=9$, episomal group, $n=6$, and mRNA/miRNA group, $n=3$, $P<0.05$). While most pluripotency markers diminished significantly to undetectable levels, *NANOG* persisted at low levels in retroviral and episomal iPSC groups at P4. The mRNA/miRNA iPSC group showed disappearance of all pluripotency markers by P4.

Discussion

The generation of iPSCs has enabled researchers to bypass the ethical concerns related to ESCs. Additional advantages of iPSCs include the ability to differentiate in vitro and produce large numbers of specific cell types and their progenitors. Therefore, there is great interest in their potential application in regenerative therapies. However, like ESCs, the tumorigenic potential of iPSCs is still a major obstacle to their application in the clinic. Generation of iPSCs from somatic cells by a delivery method without

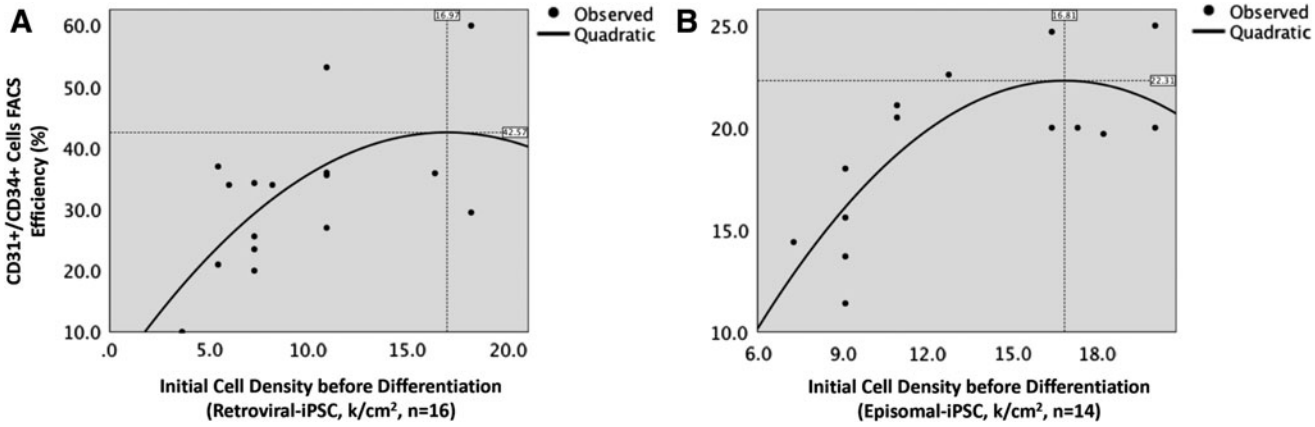

FIG. 4. Relationship between initial cell density (D) before differentiation and $CD31^+/CD34^+$ cell FACS efficiency (E) in retroviral iPSC group **(A)** and episomal iPSC group **(B)**. **(A)** Curve fitting treating density as variable and efficiency as dependent conformed to the quadratic equation: $E=1.89+4.78\times D\text{-}0.14\times D^2$. When the density was 16.97 k/cm^2, the efficiency might reach its maximum 42.57% ($n=16$, $P<0.05$). **(B)** Curve fitting conformed to the quadratic equation: $E=-7.07+3.50\times D\text{-}0.10\times D^2$. When the density was 16.81 k/cm^2, the efficiency might reach its maximum 22.31% ($n=14$, $P<0.05$).

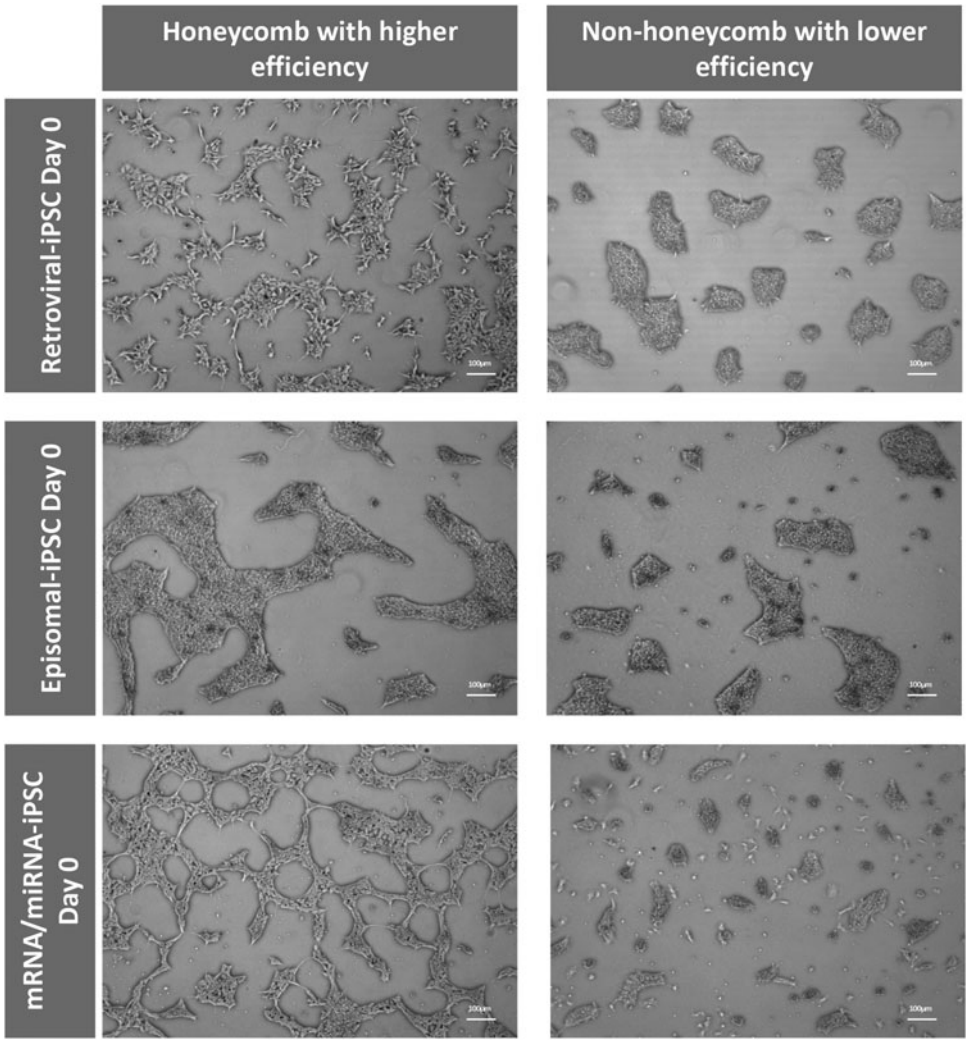

FIG. 5. The relationship between the cultured iPSC pattern on differentiation day 0 and the $CD31^+/CD34^+$ cell FACS efficiency. The differentiation runs that started out with initial cultured iPSC exhibiting the ''honeycomb'' pattern resulted in significantly higher FACS efficiency compared to those without this pattern. Scale bar = 100 μm.

exogenous tumorigenic sequences [8,21] and further differentiation into specific cell types needed for tissue regeneration [22] are strategies used to reduce the risk of tumorigenesis. However, differentiation into specific cell types is associated with inconsistent yields, which limit large-scale cell production for clinical applications.

In this study, we describe the characteristics in the differentiation of progenitor SMCs from three human iPSC lines that were reprogrammed using three different methods, including recent nonintegrative reprogramming methods. Our goals are, first, to elucidate correlations between differentiation characteristics and efficiencies that could facilitate reliable and consistent large-scale production of differentiated cells for clinical applications, and second, to examine the change in pluripotency markers in pSMCs over different passages in different iPSC lines.

We found significant correlations between starting iPSC density and differentiation efficiency that can be fitted into

TABLE 4. PERCENTAGE OF CULTURED INDUCED PLURIPOTENT STEM CELLS WITH ''HONEYCOMB'' PATTERN IN GROUPS WITH DIFFERENT EFFICIENCY

	*Lower efficiency group (*n = *5 in retroviral and episomal,* n = *3 in mRNA/miRNA)*			*Higher efficiency group (*n = *6 in retroviral and episomal,* n = *3 in mRNA/miRNA)*		
iPSC groups	*Efficiency (%)*	*Density (k/cm^2)*	*Honeycomb pattern (%)*	*Efficiency (%)*	*Density (k/cm^2)*	*Honeycomb pattern (%)*
Retroviral	20.02 ± 2.69^a	6.18 ± 0.73^b	0	38.28 ± 3.02^a	9.64 ± 1.65^b	50
Episomal	12.44 ± 1.50^a	10.18 ± 1.58^b	0	21.10 ± 0.95^a	13.03 ± 1.44^b	50
mRNA/miRNA	11.63 ± 4.37^a	30.30 ± 5.25^b	0	20.00 ± 6.09^a	30.91 ± 6.30^b	33

[a]Retroviral iPSC: $P < 0.05$, episomal iPSC: $P < 0.05$, mRNA/miRNA iPSC: $P < 0.05$.
[b]Retroviral iPSC: $P = 0.1$, episomal iPSC: $P = 0.1$, mRNA/miRNA iPSC: $P = 0.8$. Mann–Whitney test was used to verify the significance.

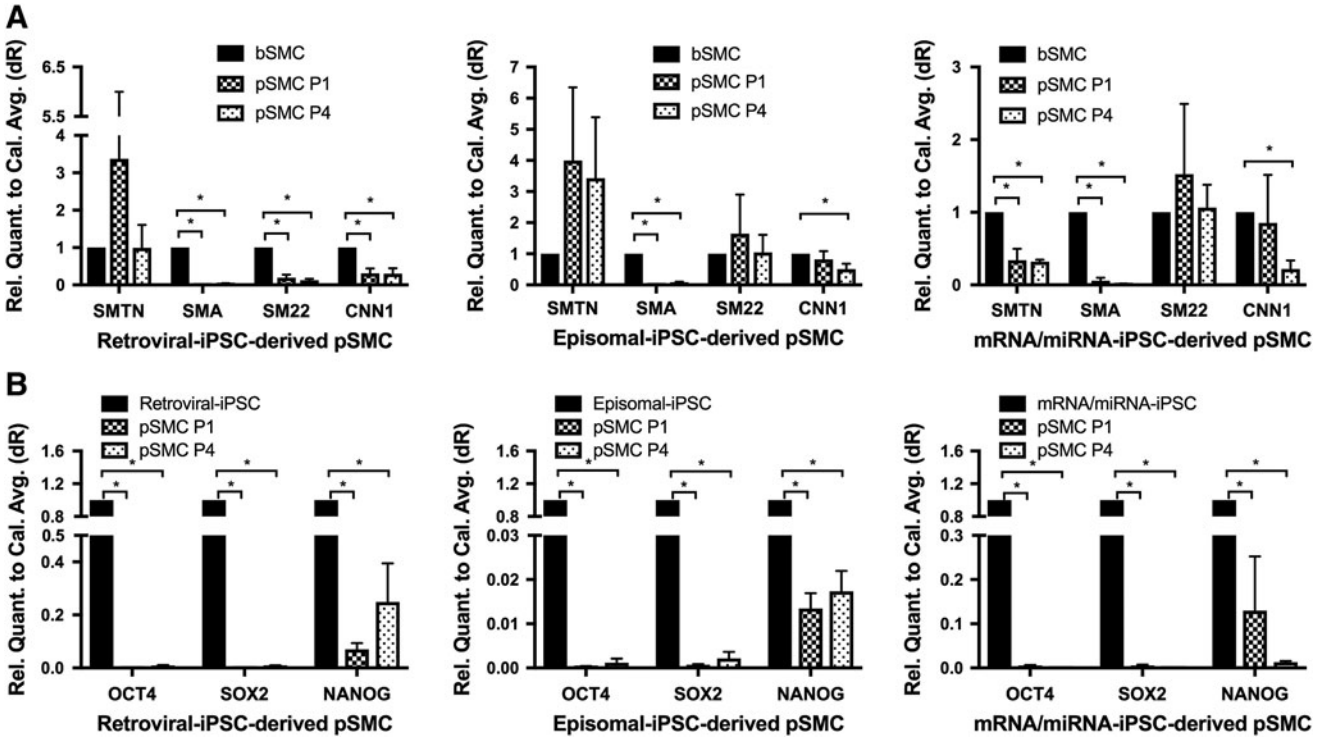

FIG. 6. Gene expression of SMC markers and pluripotency markers in passage 1 and passage 4 pSMCs and iPSCs. **(A)** Gene expression of SMC markers, including SMTN, SMA, SM22, and CNN1, in passage 1 and passage 4 pSMCs versus adult human bSMC (calibrator). Retroviral iPSC-derived pSMC, $n=9$, episomal iPSC-derived pSMC, $n=6$, and mRNA/miRNA iPSC-derived pSMC, $n=3$. **(B)** Gene expression of pluripotency markers, including OCT4, SOX2, and NANOG, in passage 1 and passage 4 pSMCs versus parental iPSC (calibrator). Retroviral iPSC-derived pSMC, $n=9$, episomal iPSC-derived pSMC, $n=6$, and mRNA/miRNA iPSC-derived pSMC $n=3$. $*P<0.05$. bSMC, adult human bladder smooth muscle cell.

quadratic equations. Interestingly, we also observed a characteristic pattern of the initial cultured iPSCs that correlates with increased differentiation efficiency. In addition, pluripotency markers decreased significantly to nearly undetectable levels in all differentiated populations, regardless of iPSC line. We believe these findings could be further optimized to facilitate large-scale production of cells and ongoing efforts to translate stem cell technologies into regenerative therapies.

The $CD31^+/CD34^+$ cell FACS efficiency is defined as the percentage yield of $CD31^+/CD34^+$ cells from the cell population undergoing differentiation. Higher efficiencies are essential for the production of large cell doses required for clinical applications. In this study, we found that the $CD31^+/CD34^+$ cell FACS efficiency increased with starting iPS cell density up to an optimum limit. This relationship was best described by a quadratic curve. This quadratic equation, which is specific to each iPSC line, can be used to predict the efficiency at a given starting iPSC density for process surveillance. More importantly, these equations can be used to predict the most suitable initial cell density range to obtain maximum yield of differentiated cells for large-scale production.

In addition to initial cell density, $CD31^+/CD34^+$ cell FACS efficiency was also associated with the iPS cell growth pattern (''honeycomb-like'' appearance) on Matrigel on day 0 of the differentiation process. We observed that cell cultures exhibiting this honeycomb-like pattern differentiated more efficiently with higher yields (significant difference compared to those cultures without this pattern), suggesting that this pattern may also be used to predict efficiency. We hypothesize that there are underlying reasons such as cell-to-cell interaction and matrix biomechanical properties that contribute to this pattern. Further studies to elucidate these mechanisms are needed.

For therapeutic application of stem cell-derived cells, purification methods should also be considered. Differentiation of iPSCs into pSMCs invariably results in subpopulations that may include undifferentiated cells and different stages of muscle cells [22]. Quantitative PCR was used to detect relative gene expression of SMCs and pluripotency markers to examine SMC phenotype of cells differentiated from the different iPSC lines after purification, and whether this phenotype changed over time with cell expansion.

SMTN is found only in the tissue of internal organs, urogenital tract, and vascular SMCs [23,24]. It co-localizes with α-SMA stress fibers in the cytoskeleton and plays an important role in SMC contractility [25]. The expression of SMTN distinguishes the contractile SMCs from myofibroblasts, which only express SMA [26]. The expression of smoothelin in retroviral and episomal iPSC-derived pSMCs in our study was similar to that in adult human bladder SMCs. The expression of smoothelin and SMA in mRNA-/miRNA-derived pSMCs was lower than that in adult bladder SMCs. This variability in SMC marker profile expression suggests that the pSMCs from different lines may not be at the same stage of progenitor differentiation at the same passage. Further studies are needed to determine if this variability is due to reprogramming method or patient-to-patient differences.

SMA is reported to be an early marker in SMC development and its expression was detected after 3 weeks of differentiation in conjunction with SMTN [27]. Our differentiation protocol uses PDGF-BB to induce $CD31^+/CD34^+$ VPCs seeded on collagen IV-coated plates into smooth muscle progenitor cells [14]. PDGF-BB is a potent mitogenic factor and has been demonstrated to suppress expression of α-SMA with IL-1 in mature SMCs [28]. This function keeps pSMCs from completing their differentiation to mature functional SMCs by inhibiting the expression of SMC markers [29]. In this study, we found that the relative expression of SMA in all iPSC-derived pSMCs was significantly lower than in adult bladder SMCs. This finding and the presence of Ki67, a marker for proliferation, are consistent with a progenitor phenotype.

Pluripotency markers are indicators for maintenance of pluripotency, which increases the potential for tumor formation. Published data suggest that OCT4, SSEA3, and TRA-1-60 are the most sensitive to differentiation signals and can be used to validate pluripotent stem cell pluripotency [30]. SSEA3, SSEA4, TRA-1-60, and TRA-1-81 are cell surface pluripotent markers for stem cells, while OCT4, NANOG, and alkaline phosphatase (AP) are intracellular markers. We used these markers to evaluate if there are cell populations with pluripotency phenotypes in our final pSMC populations.

In our study, TRA-1-60 and TRA-1-81 were negative in all pSMCs regardless of iPSC line. This was accompanied by successful differentiation, confirmed by the positive expression of SMC markers (SMTN, SMA, SM22, and CNN1) in pSMCs. SOX2 is an essential transcription factor for keeping stem cells in a pluripotent state. It is suggested that the presence of SOX2 forces the expression of OCT4 protein indirectly, which activates the OCT-SOX enhancer next to keep stem cells in the pluripotent state [31]. OCT-SOX enhancers can promote the expression of OCT4, SOX2, and NANOG [32,33]. Therefore, NANOG is not an essential gene for generation of iPSCs, but acts as a core factor in the pluripotency regulatory network [7]. Ramirez, et al. documented that, during mesoderm differentiation of human ESCs, the expression of SSEA3, OCT4, and TRA-1-60 is lost earlier and more rapidly than the other markers, while other pluripotent markers such as CD24, AP, and NANOG persisted on day 9 [30]. Our data are consistent with this, in that, the intracellular pluripotency markers OCT4, SOX2, and NANOG were detected in extremely low levels in the P4 pSMC groups from retroviral and episomal reprogrammed iPSC lines. However, these were all nondetectable in the mRNA-/miRNA-reprogrammed iPSC-derived P4 pSMCs, suggesting that mRNA/miRNA iPSCs may be more efficient at losing pluripotency characteristics during differentiation. In vivo studies will be needed to determine whether these low-level differences in NANOG have a tumorigenic effect.

There was no difference in SMC marker expression (SMTN, SMA, SM22, and CNN1) between P1 and P4 pSMCs. The same held true for pluripotency marker expression (OCT4, SOX2, and NANOG) between passages 1 and 4. Thus, the SMC phenotype did not change through extensive passaging of pSMCs. Taken together, it appears that different iPSC reprogramming methods did not affect the cell's ability to differentiate in vitro or the stability of the resulting pSMC population. Differences in iPSC starting density and differentiation efficiency curve fitting formulas may be related to patient-specific genetic determinants. Larger numbers of iPSC lines are needed to confirm this.

Conclusion

Human iPSC lines, each derived with different iPSC reprogramming methods, differentiated into smooth muscle progenitor cells using the same protocol. The iPSC density at the start of differentiation correlated with the $CD31^+/CD34^+$ cell FACS efficiency. In addition, a ''honeycomb'' pattern of the cultured iPS cells at the beginning of differentiation was associated with higher differentiation efficiency. Expression of pluripotency markers in early- and late-passage pSMC populations was minimal and similar between the three iPSC-derived groups, suggesting stable cell populations through cell expansion methods. These findings can be used to optimize large-scale production of iPSC-derived cells for clinical therapies.

Acknowledgment

This study was supported by grants from the California Institute of Regenerative Medicine (CIRM) TR3-05569 and DISC1-08731.

Author Disclosure Statement

The authors have no financial conflict of interests in the content of this article.

References

1. Harding A, E Cortez-Toledo, NL Magner, JR Beegle, DP Coleal-Bergum, D Hao, A Wang, JA Nolta and P Zhou. (2017). Highly efficient differentiation of endothelial cells from pluripotent stem cells requires the MAPK and the PI3K pathways. Stem Cells 35:909–919.
2. Maguire EM, Q Xiao and Q Xu. (2017). Differentiation and application of induced pluripotent stem cell-derived vascular smooth muscle cells. Arterioscler Thromb Vasc Biol 37:2026–2037.
3. Li Y, M Green, Y Wen, Y Wei, P Wani, Z Wang, R Reijo Pera and B Chen. (2017). Efficacy and safety of immunomagnetically sorted smooth muscle progenitor cells derived from human-induced pluripotent stem cells for restoring urethral sphincter function. Stem Cells Transl Med 6:1158–1167.
4. Wang Z, Y Wen, YH Li, Y Wei, M Green, P Wani, P Zhang, RR Pera and B Chen. (2016). Smooth muscle precursor cells derived from human pluripotent stem cells for treatment of stress urinary incontinence. Stem Cells Dev 25:453–461.
5. Takahashi K, K Tanabe, M Ohnuki, M Narita, T Ichisaka, K Tomoda and S Yamanaka. (2007). Induction of pluripotent stem cells from adult human fibroblasts by defined factors. Cell 131:861–872.
6. Yu J, MA Vodyanik, K Smuga-Otto, J Antosiewicz-Bourget, JL Frane, S Tian, J Nie, GA Jonsdottir, V Ruotti, et al. (2007). Induced pluripotent stem cell lines derived from human somatic cells. Science 318:1917–1920.
7. Yoshida Y and S Yamanaka. (2017). Induced pluripotent stem cells 10 years later: for cardiac applications. Circ Res 120:1958–1968.
8. Yu J, K Hu, K Smuga-Otto, S Tian, R Stewart, II Slukvin and JA Thomson. (2009). Human induced pluripotent stem

cells free of vector and transgene sequences. Science 324: 797–801.
9. Lin SL, DC Chang, CH Lin, SY Ying, D Leu and DT Wu. (2011). Regulation of somatic cell reprogramming through inducible mir-302 expression. Nucleic Acids Res 39:1054–1065.
10. Miyoshi N, H Ishii, H Nagano, N Haraguchi, DL Dewi, Y Kano, S Nishikawa, M Tanemura, K Mimori, et al. (2011). Reprogramming of mouse and human cells to pluripotency using mature microRNAs. Cell Stem Cell 8:633–638.
11. Anokye-Danso F, CM Trivedi, D Juhr, M Gupta, Z Cui, Y Tian, Y Zhang, W Yang, PJ Gruber, JA Epstein and EE Morrisey. (2011). Highly efficient miRNA-mediated reprogramming of mouse and human somatic cells to pluripotency. Cell Stem Cell 8:376–388.
12. Barral S, J Ecklebe, S Tomiuk, MC Tiveron, A Desoeuvre, D Eckardt, H Cremer and A Bosio. (2013). Efficient neuronal in vitro and in vivo differentiation after immunomagnetic purification of mESC derived neuronal precursors. Stem Cell Res 10:133–146.
13. Borchin B, J Chen and T Barberi. (2013). Derivation and FACS-mediated purification of PAX3+/PAX7+ skeletal muscle precursors from human pluripotent stem cells. Stem Cell Rep 1:620–631.
14. Marchand M, EK Anderson, SM Phadnis, MT Longaker, JP Cooke, B Chen and RA Reijo Pera. (2014). Concurrent generation of functional smooth muscle and endothelial cells via a vascular progenitor. Stem Cells Transl Med 3:91–97.
15. Lian X, X Bao, A Al-Ahmad, J Liu, Y Wu, W Dong, KK Dunn, EV Shusta and SP Palecek. (2014). Efficient differentiation of human pluripotent stem cells to endothelial progenitors via small-molecule activation of WNT signaling. Stem Cell Rep 3:804–816.
16. Seabright M. (1971). A rapid banding technique for human chromosomes. Lancet 2:971–972.
17. Wang C, X Tang, X Sun, Z Miao, Y Lv, Y Yang, H Zhang, P Zhang, Y Liu, et al. (2012). TGFbeta inhibition enhances the generation of hematopoietic progenitors from human ES cell-derived hemogenic endothelial cells using a stepwise strategy. Cell Res 22:194–207.
18. Wen Y, P Wani, L Zhou, T Baer, SM Phadnis, RA Reijo Pera and B Chen. (2013). Reprogramming of fibroblasts from older women with pelvic floor disorders alters cellular behavior associated with donor age. Stem Cells Transl Med 2:118–128.
19. Li Y, Y Wen, M Green, EK Cabral, P Wani, F Zhang, Y Wei, TM Baer and B Chen. (2017). Cell sex affects extracellular matrix protein expression and proliferation of smooth muscle progenitor cells derived from human pluripotent stem cells. Stem Cell Res Ther 8:156.
20. Bajpai VK, P Mistriotis, YH Loh, GQ Daley and ST Andreadis. (2012). Functional vascular smooth muscle cells derived from human induced pluripotent stem cells via mesenchymal stem cell intermediates. Cardiovasc Res 96: 391–400.
21. Warren L, PD Manos, T Ahfeldt, YH Loh, H Li, F Lau, W Ebina, PK Mandal, ZD Smith, et al. (2010). Highly efficient reprogramming to pluripotency and directed differentiation of human cells with synthetic modified mRNA. Cell Stem Cell 7: 618–630.
22. Ghosh Z, M Huang, S Hu, KD Wilson, D Dey and JC Wu. (2011). Dissecting the oncogenic and tumorigenic potential of differentiated human induced pluripotent stem cells and human embryonic stem cells. Cancer Res 71:5030–5039.
23. van Eys GJ, MC Völler, ED Timmer, XH Wehrens, JV Small, JA Schalken, FC Ramaekers and FT van der Loop. (1997). Smoothelin expression characteristics: development of a smooth muscle cell in vitro system and identification of a vascular variant. Cell Struct Funct 22: 65–72.
24. van der Loop FT, G Schaart, ED Timmer, FC Ramaekers and GJ van Eys. (1996). Smoothelin, a novel cytoskeletal protein specific for smooth muscle cells. J Cell Biol 134: 401–411.
25. Niessen P, S Rensen, J van Deursen, J De Man, A De Laet, JM Vanderwinden, T Wedel, D Baker, P Doevendans, et al. (2005). Smoothelin-a is essential for functional intestinal smooth muscle contractility in mice. Gastroenterology 129: 1592–1601.
26. Tomasek JJ, G Gabbiani, B Hinz, C Chaponnier and RA Brown. (2002). Myofibroblasts and mechano-regulation of connective tissue remodelling. Nat Rev Mol Cell Biol 3: 349–363.
27. Salem SA, AN Hwie, A Saim, CH Chee Kong, I Sagap, R Singh, MR Yusof, Z Md Zainuddin and R Hj Idrus. (2013). Human adipose tissue derived stem cells as a source of smooth muscle cells in the regeneration of muscular layer of urinary bladder wall. Malays J Med Sci 20:80–87.
28. Chen CN, YS Li, YT Yeh, PL Lee, S Usami, S Chien and JJ Chiu. (2006). Synergistic roles of platelet-derived growth factor-BB and interleukin-1beta in phenotypic modulation of human aortic smooth muscle cells. Proc Natl Acad Sci U S A 103:2665–2670.
29. Lin C, Y Yuan and DW Courtman. (2016). Differentiation of Murine Bone Marrow-Derived Smooth Muscle Progenitor Cells Is Regulated by PDGF-BB and Collagen. PLoS One 11:e0156935.
30. Ramirez JM, S Gerbal-Chaloin, O Milhavet, B Qiang, F Becker, S Assou, JM Lemaître, S Hamamah and J De Vos. (2011). Brief report: benchmarking human pluripotent stem cell markers during differentiation into the three germ layers unveils a striking heterogeneity: all markers are not equal. Stem Cells 29:1469–1474.
31. Masui S, Y Nakatake, Y Toyooka, D Shimosato, R Yagi, K Takahashi, H Okochi, A Okuda, R Matoba, et al. (2007). Pluripotency governed by Sox2 via regulation of Oct3/4 expression in mouse embryonic stem cells. Nat Cell Biol 9: 625–635.
32. Boyer LA, TI Lee, MF Cole, SE Johnstone, SS Levine, JP Zucker, MG Guenther, RM Kumar, HL Murray, et al. (2005). Core transcriptional regulatory circuitry in human embryonic stem cells. Cell 122:947–956.
33. Loh YH, Q Wu, JL Chew, VB Vega, W Zhang, X Chen, G Bourque, J George, B Leong, et al. (2006). The Oct4 and Nanog transcription network regulates pluripotency in mouse embryonic stem cells. Nat Genet 38:431–440.

Address correspondence to:
Dr. Yan Wen
Department of Obstetrics/Gynecology
Stanford University School of Medicine
300 Pasteur Drive HH-333
Stanford, CA, 94305

E-mail: yanwen@stanford.edu

Received for publication February 7, 2018
Accepted after revision July 23, 2018
Prepublished on Liebert Instant Online XXXX XX, XXXX